Clinical Imaging 51 (2018) 68–75

Contents lists available at ScienceDirect

Clinical Imaging

journal homepage: www.elsevier.com/locate/clinimag

Value of ^{18}F-FET PET in adult brainstem glioma

Abdulrahman Abdullah Albatly[a,b], Adnan Taleb Alsamarah[a,c,d], Abdulrahman Alhawas[a,e], Patrick Veit-Haibach[a], Alfred Buck[a], Paul Stolzmann[a], Irene A. Burger[a], Spyros S. Kollias[c], Martin W. Huellner[a,c,*]

[a] Department of Nuclear Medicine, University Hospital Zurich/University of Zurich, Rämistrasse 100, 8091 Zurich, Switzerland
[b] Department of Diagnostic Radiology, Prince Sultan Medical Military City, Makkah Road, Riyadh, Saudi Arabia
[c] Department of Neuroradiology, University Hospital Zurich/University of Zurich, Frauenklinikstrasse 10, 8091 Zurich, Switzerland
[d] Department of Diagnostic Radiology, King Fahd University Hospital, Onizah Street, Alkhobar, Saudi Arabia
[e] Department of Radiology and Medical Imaging, College of Medicine, King Saud University, Riyadh, Saudi Arabia

ARTICLE INFO

Keywords:
Adult brainstem glioma
^{18}F-FET
PET
Tyrosin
PET/CT
Brain tumors
MR
PET/MR
Survival
Kaplan-Meier

ABSTRACT

Purpose: To investigate ^{18}F-fluoro-ethyl-tyrosine positron emission tomography (FET-PET) imaging characteristics of adult brainstem glioma (BSG).

Materials and methods: FET-PET imaging and progression-free survival (PFS) of 16 adult patients with BSG was analyzed (9 high-grade gliomas, 7 low-grade gliomas). SUV_{max}, TBR, and time activity curves of FET-PET were calculated.

Results: Progressive gliomas had higher SUV_{max} (3.57 ± 1.47 vs. 1.60 ± 0.51; $p = 0.003$) and TBR_{max} (3.00 ± 1.12 vs. 1.36 ± 0.33; $p = 0.001$) than stable gliomas. Kaplan-Meier analysis showed longer PFS of tumors with $TBR_{max} < 2.0$ compared to tumors with $TBR_{max} > 2.0$ (665 ± 32 days versus 220 ± 39 days; $p < 0.001$).

Conclusion: FET-PET uptake might be associated with disease progression in adult BSG.

1. Introduction

Brainstem tumors are defined as neoplastic lesions arising in the midbrain, the pons, or the medulla oblongata [1,2]. Brainstem gliomas (BSG) are a heterogeneous group of gliomas with a bimodal age distribution, occurring predominantly in children and young adults. Compared to children, BSG are rare in adults, accounting for only 1–2% of all adult primary glial neoplasms [3]. They represent a diverse group of tumors with varying radiological appearance and prognosis that differs from BSG occurring in the pediatric age group [4]. Adult BSG show a tendency towards a biphasic age distribution, with a first peak in the third decade of life and a second peak in the sixth decade [5]. A low-grade phenotype predominates in adults, being one feature that possibly explains their better survival compared to children [6].

Magnetic resonance (MR) imaging is the diagnostic method of choice for BSG [7]. Four different subgroups of BSG are identified based on their MR imaging characteristics: (a) diffuse intrinsic low-grade gliomas, (b) enhancing malignant gliomas, (c) focal tectal gliomas and (d) exophytic gliomas/other subtypes [8]. Unlike supratentorial gliomas, even high-grade BSG oftentimes lack contrast enhancement. Necrosis is very uncommon in adult BSG, while exophytic growth is uncommon in supratentorial gliomas.

Supratentorial gliomas are often examined using complementary MR techniques such as MR spectroscopy (MRS) to determine the histologic grade of the lesion [9]. However, the use of MRS is limited in the brainstem due to technical difficulties, such as low signal-to-noise ratio, small size of structures, and proximity of cancellous bone and bone marrow [8,9].

Due to their delicate location, biopsy is infrequently performed in BSG, and treatment and frequency of follow-up is often based on their classification by MR.

Owing to availability issues, the worldwide most commonly used

Abbreviations: ADC, apparent diffusion coefficient; BSG, brain stem glioma; Cho, choline; CT, computed tomography; DTI, diffusion tensor imaging; DWI, diffusion weighted imaging; FET, ^{18}F-fluoro-ethyl-tyrosine; FLAIR, fluid-attenuated inversion recovery; GBM, glioblastoma multiforme; IDH, isocitrate dehydrogenase; KFS, Karnofsky performance status; LOH, loss of heterozygosity; MCP, middle cerebellar peduncle; MGMT, O(6)-methlyguanine-DNA-methyltransferase; MR, magnetic resonance; MRS, magnetic resonance spectroscopy; NAA, *N*-acetylaspartate; PET, positron emission tomography; PFS, progression-free survival; PWI, perfusion-weighted imaging; RT, radiation therapy; SUV_{max}, maximum standardized uptake value; T1w, T1-weighted; T2w, T2-weighted; TAC, time activity curve; TBR, tumor-to-brain ratio; TMZ, temozolomide; VOI, volume of interest; WM, white matter

* Corresponding author at: Department of Nuclear Medicine, University Hospital Zurich/University of Zurich, Rämistrasse 100, 8091 Zurich, Switzerland.
E-mail addresses: aalhawas1@ksu.edu.sa (A. Alhawas), patrick.veit-haibach@usz.ch (P. Veit-Haibach), fred.buck@usz.ch (A. Buck), paul.stolzmann@usz.ch (P. Stolzmann), irene.burger@usz.ch (I.A. Burger), spyros.kollias@usz.ch (S.S. Kollias), martin.huellner@usz.ch (M.W. Huellner).

https://doi.org/10.1016/j.clinimag.2018.01.015
Received 27 October 2017; Received in revised form 25 January 2018; Accepted 29 January 2018

radiotracer in BSG patients today remains fluorodeoxyglucose — despite limitations due to high physiologic uptake of normal brain tissue [10–12]. Amino acid tracer imaging, such as ^{18}F-fluoro-ethyl-tyrosine positron emission tomography (FET-PET), is a well-investigated imaging modality for supratentorial tumors. A number of studies have proven the clinical value of amino acid tracers, such as FET, to determine the extent of cerebral gliomas for treatment planning and biopsy guidance, the detection of tumor recurrence and the estimation of prognosis [13].

Besides the standardized maximum uptake value (SUV_{max}), ^{18}F-FET imaging uses tumor-to-background ratios (TBR). TBR is defined as the ratio of the lesion's SUV and the mean SUV of healthy supratentorial brain tissue [14,15]. TBR_{max} can distinguish high-grade supratentorial glioma and lymphoma from low-grade supratentorial glioma and non-neoplastic lesions using a threshold of 2.5 [16–18].

FET-PET might represent a useful adjunct to MR imaging of BSG, especially since metabolic information derived by advanced MR techniques is unsatisfactory in the brainstem. Recently, Tscherpel et al. could show in a mixed population of adult and pediatric BSG and spinal cord gliomas that FET uptake is increased (TBR > 2.5) in high-grade lesions as well as in a considerable number of low-grade lesions [19]. Specific data exists about amino acid PET in children with diffuse-intrinsic low-grade BSG subtype, where ^{11}C-methionine PET failed to show a distinct uptake pattern [10,20]. FET-PET might also provide complementary information on the survival of patients. According to Tscherpel et al., FET-PET might be able to identify progression of BSG/spinal cord gliomas by using a combination of TBR and dynamic uptake parameters [19]. Lack of amino acid uptake in low-grade BSG in children might be associated with improved survival, as was shown for ^{11}C-methionine PET [10]. Despite a few recent publications on FET-PET in infratentorial tumors, specific data on ^{18}F-FET characteristics of adult BSG, their relation to specific MR phenotypes, and their possible value for the prognostication of patient survival are still scarce in the literature.

The purpose of our study was to identify FET-PET characteristics of low-grade and high-grade adult BSG, and to analyze the ability of FET-PET to prognosticate survival.

2. Material and methods

This retrospective study was approved by the local ethics committee, and has therefore been performed in accordance with the ethical standards laid down in the 1964 Declaration of Helsinki and its later amendments. For retrospective studies, our institution uses a general consent form all patients are provided with upon admission since 2014. Patients with documented refusal of consent were not enrolled in our study. Informed consent was waived for patients scanned before 2014. FET-PET is a clinically validated and partly reimbursed imaging modality for brain tumor patients (including BSG) in our country.

2.1. Clinical data

Our institution is a tertiary referral university hospital that serves as a national reference center for the treatment of adult brain tumors. The inclusion criteria for our study consisted of a FET-PET scan acquired for the work-up of BSG in clinically stable patients, availability of at least one contrast-enhanced MR exam within 6 weeks of the PET scan, and absence of therapy or intervention between these two exams. A full-text search in the picture archiving and communication system (PACS) of our institution, using the terms “brainstem”, “infratentorial”, “pons”, “mesencephalon”, “medulla oblongata” in conjunction with the terms “glioma”, “tumor”, “neoplasm”, and covering the period from January 2010 to December 2016, revealed 16 patients with an adult BSG, who met the inclusion criteria. The diagnosis of BSG was based on histopathology in 9 patients (56.3%), and on MR imaging characteristics and clinical follow-up in 7 patients (43.7%). We collected clinical and demographic data of patients (age, sex, and indication of scan), history of therapy before scan, and available histopathology, including data on molecular markers of tumors.

In each patient, the progression-free survival (PFS) was determined. Progression was defined as tumor growth on FLAIR-weighted images (> 10%), new onset contrast-enhancement on MR, worsening clinical symptoms requiring tumor-specific therapy, failure to return for follow-up because of deteriorating condition or death (if not caused by an unrelated disorder). Hence, stability was defined as absence of clinical signs and imaging signs of progression. We did not exactly use RANO criteria for glioblastoma or diffuse low-grade glioma, since these criteria deal with supratentorial gliomas [21,22]. Currently, no validated response criteria exist for BSG. RANO criteria for supratentorial gliomas cannot be directly transferred to BSG in our opinion, e.g. tumor growth by < 25% would imply stable disease according to RANO, but a BSG patient might already suffer from severe signs of progression such as occlusive hydrocephalus at this time point, owing to the delicate tumor location. However, we used criteria which reflect clinical routine assessment of BSG, and which are very similar to RANO.

2.2. Image analysis

We analyzed the first FET-PET scan available in every patient, and the MR scan closest to this FET-PET scan.

2.2.1. MR imaging

On MR, the following criteria were assessed: tumor location, tumor size in three dimensions on fluid-attenuated inversion recovery (FLAIR)-weighted images, presence of contrast enhancement on T1-weighted (T1w) pre-contrast and post-contrast images, presence of perifocal edema on T2-weighted (T2w) images, and presence of restricted diffusion and apparent diffusion coefficient (ADC) values on diffusion-weighted imaging (DWI). MR exams were carried out on different 3 Tesla scanners. Based on their imaging characteristics, all BSG were classified into 4 types (diffuse intrinsic low-grade glioma, enhancing malignant glioma, focal tectal glioma and exophytic glioma/other subtypes) [8].

2.2.2. FET-PET imaging

FET-PET is acquired in a standardized way at our institution. Exams were obtained on a Discovery ST 16 scanner (GE Healthcare, Waukesha WI), on a Discovery VCT scanner (GE Healthcare), or on a Discovery 690 Standard scanner (GE Healthcare). According to our institution's protocols, patients were injected with a standardized dose of 130 MBq of ^{18}F-FET (median: 131 MBq, range 110–150 MBq). Dynamic FET-PET acquisition started 20 min after radiotracer injection, with four 5 min frames, covering a total acquisition time of 20 min [19,23]. Static PET images of the whole 20 min acquisition scan were reconstructed from raw data. Emission data were corrected in a standardized way (randoms, dead time, scatter, attenuation). The attenuation-corrected axial PET datasets were iteratively reconstructed with a matrix size of 128 × 128 pixels (voxel spacing: 2.3438 ∗ 2.3438 ∗ 3.27). All FET-PET data analyses used dedicated software (PMOD® 3.7, PMOD technologies, Zürich, Switzerland). This software also allows for retrospective co-registration of FET and MR image datasets.

The following FET-PET parameters were investigated: SUV_{max}, TBR and time activity curve (TAC) pattern. The calculation of SUV_{max} and TBR used the static PET dataset mentioned above. For defining the SUV_{max}, the average of the 5 hottest voxels of the lesion was used, according to vendor's suggestions. These suggestions are based on potential intratumoral heterogeneity, and have been devised to reduce dependency from a single voxel value [24–27]. TBR was calculated by dividing the SUV_{max} of the tumor by the SUV_{mean} of the normally appearing superior parietal lobule, including gray and white matter. This (supratentorial) area was chosen because no specific reference region

exists for BSG. Other authors used a similar reference region for TBR calculation [19,28–30].

Based on the slope of the TAC derived from the dynamic PET dataset, different patterns were assigned [31]:

- Pattern 1 (wash-in) = change > +10% during the aforementioned four 5 min frames
- Pattern 2 (plateau) = change ± 10%
- Pattern 3 (wash-out) = change < −10%.

Additionally, as suggested by Pöpperl and coworkers, the sum of the frame-to-frame differences in SUV_{max} was calculated: $\Sigma(n_i - n_{i-1})$ [32].

2.3. Histopathology

In nine patients who underwent biopsy, tumors were categorized according to the world health organization (WHO) classification of tumors of the central nervous system [33]. In 9 patients, where enough tissue was provided for histopathology, one or more of the following molecular biomarkers were routinely analyzed: O(6)-methlyguanine-DNA-methyltransferase (MGMT) promoter methylation, loss of heterozygosity (LOH) of chromosomes 1p and 19q, and isocitrate dehydrogenase (IDH) (types 1 and 2) mutations. If these analyses had been carried out, data was recorded for our study, too.

2.4. Statistical analysis

Ordinal non-dichotomous variables are expressed as median (with range), nominal non-dichotomous variables are expressed as mode (percentage), and ratio variables are expressed as geometric mean ± standard deviation. FET characteristics among different types of BSG (according to MR appearance and histopathology) and among progressive and stable tumors were compared using Mann-Whitney *U* test. Survival analyses were performed using Kaplan-Meier statistics. The difference of survival distributions among different types of BSG (according to MR appearance and histopathology) and among progressive and stable tumors was tested for significance using a log rank test (Mantel Cox). A p-value of < 0.05 was deemed statistically significant. Statistical analysis used SPSS® version 22 (IBM, Armonk, NY).

3. Results

Our cohort consisted of 12 male and 4 female patients (median age 32 years; range 16–51 years). Detailed information on demographics are given in Table 1. The median time interval between FET-PET and MR imaging was 9 days (range 0–42 days; all patients with an interval of > 20 days had low-grade gliomas). The majority of patients had a KPS of ≥90 at the time of diagnosis (Table 1). Most patients (12 of 16, 75.0%) had no history of previous therapy. In these patients, the tumor was diagnosed incidentally on MRI. The other 4 patients had previous radiotherapy and chemotherapy with temozolomide (TMZ), and they were also clinically stable at the time of FET-PET imaging.

Histopathology was available in 9 patients (56.3%), with the most common histopathological tumor type being anaplastic astrocytoma (WHO III) (Table 1). LOH was negative in 4 patients; IDH1 was wild type variant in 5 patients and mutated variant in 1 patient; IDH2 was wild type variant in 4 patients and mutated variant in 1 patient; and the MGMT promoter was methylated in 2 patients and not methylated in another 2 patients. In the remaining patients, no data on molecular markers was available. Altogether, data on molecular markers was too sparse and heterogeneous to allow for a conclusive analysis.

Most tumors had a combined location in the medulla oblongata and the pons, with a mean tumor size of 38 mm ± 13 mm on FLAIR-weighted images. Data on MR features of tumors are given in (Table 2). The majority of tumors (9 of 16, 56.3%) were classified as diffuse

Table 1
Patient demographics, clinical condition and tumor histopathology.

Total patients (n)	16
Males (n (%))	12 (75.0%)
Females (n (%))	4 (25.0%)
Age (median (range))	33 (16–51)
16–21 years (n (%))	1 (6.3%)
22–39 years (n (%))	11 (68.7%)
40–51 years (n (%))	4 (25.0%)
KPS at time of FET-PET (median (range))	90 (70–100)
100 (n (%))	5 (31.0%)
90 (n (%))	6 (37.5%)
80 (n (%))	3 (18.8%)
70 (n (%))	2 (12.5%)
Histopathologic diagnosis	
Glioblastoma (WHO IV) (n (%))	1 (6.3%)
Anaplastic astrocytoma (WHO III) (n (%))	6 (37.5%)
Low-grade astrocytoma (WHO II) (n (%))	2 (12.5%)
No biopsy (n (%))	7 (43.7%)

Note — FET, ^{18}F-fluoro-ethyl-tyrosine; KPS, Karnofsky performance status; WHO, World Health Organization.

Table 2
MR imaging characteristics of tumors.

MRI-based tumor classification	
Diffuse intrinsic low-grade glioma (n (%))	9 (56.3%)
Enhancing malignant glioma (n (%))	5 (31.3%)
Focal tectal glioma (n (%))	1 (6.2%)
Exophytic glioma (n (%))	1 (6.2%)
Tumor location	
Medulla oblongata (n (%))	3 (18.75%)
Medulla oblongata + pons (n (%))	6 (37.50%)
Pons (n (%))	1 (6.25%)
Tectum (n (%))	1 (6.25%)
Midbrain, pons, brachium pontis (n (%))	1 (6.25%)
Cisterna pontocerebellaris/cisterna cerebellomedullaris lateralis (n (%))	1 (6.25%)
Midbrain, pons (n (%))	1 (6.25%)
Midbrain (n (%))	1 (6.25%)
Pons, cerebellum, medulla oblongata (n (%))	1 (6.25%)
Presence of contrast enhancement	
Yes (n (%))	5 (31.3%)
No (n (%))	11 (68.7%)
Tumor size on FLAIR (longest diameter [mm])	
All tumors (mean ± SD)	38 ± 13
Enhancing malignant glioma (mean ± SD)	32 ± 8
Diffuse intrinsic low-grade glioma (mean ± SD)	44 ± 14
Presence of peritumoral edema	
Yes (n (%))	6 (37.5%)
No (n (%))	10 (62.5%)
ADC map signal	
Bright (n (%))	11 (68.8%)
Dark (n (%))	2 (12.5%)
Mixed (n (%))	3 (18.7%)

Note — ADC, apparent diffusion coefficient; FLAIR, fluid-attenuated inversion recovery; SD standard deviation.

Table 3
FET-PET characteristics of tumors, stratified by MR appearance.

SUV_{max}	
Diffuse intrinsic low-grade glioma (mean ± SD)	3.11 ± 1.60
Enhancing malignant glioma (mean ± SD)	3.02 ± 1.04
Focal tectal glioma	1.20
Exophytic glioma	0.85
TBR_{max}	
Diffuse intrinsic low-grade glioma (mean ± SD)	2.54 ± 1.35
Enhancing malignant glioma (mean ± SD)	2.56 ± 0.57
Focal tectal glioma	1.20
Exophytic glioma	0.92
FET time activity curve	
Pattern 1: wash-in (n (%))	2 (12.5)
Pattern 2: plateau (n (%))	5 (31.25)
Pattern 3: wash-out (n (%))	9 (56.25)

Note — FET, ^{18}F-fluoro-ethyl-tyrosine; SUV_{max}, maximum standardized uptake value; TBR_{max}, tumor-to-brain ratio.

intrinsic low-grade glioma (Table 2). Detailed data on FET-PET characteristics of tumors, stratified by their MR appearance, is given in (Table 3).

Based on histopathology, BSG were divided into low-grade tumors (WHO II; Fig. 1) and high-grade tumors (WHO III and IV; Fig. 2). If histopathology was unavailable – being a common issue in BSG – then their MR appearance was used as a surrogate to designate them as low-grade lesions or high-grade lesions.

SUV_{max} and TBR_{max} were not significantly different between high-grade gliomas (HGG) and low-grade gliomas (LGG) ($p = 0.711$, $p = 0.672$, respectively) (Table 4). The TAC analysis demonstrated an overlap between HGG and LGG, without significant difference of the uptake at all TAC points (t) (p-values: 0.758 (t1), 1.000 (t2), 0.918 (t3), 0.758 (t4) (Fig. 3A)).

Progressive gliomas ($n = 11$) showed significantly higher SUV_{max} and TBR_{max} compared to stable gliomas ($n = 5$) ($p = 0.003$, $p = 0.001$, respectively) (Table 4). The TAC analysis showed significantly higher uptake of progressive gliomas than stable gliomas at all time points (t) (p-values: 0.003 (t1), 0.007 (t2), 0.007 (t3), 0.005 (t4) (Fig. 3B)).

Overall, five patients (31.3%) remained clinically stable during a follow-up period of 389 to 641 days (mean 479 days). BSG was confirmed by histopathology in four of them. The remaining 11 patients (68.7%) had disease progression after a mean PFS of 298 ± 195 days.

Kaplan-Meier analysis showed a somewhat earlier progression of HGG than LGG. However, this trend did not reach statistical significance, and PFS was equal among HGG and LGG (Fig. 4A). PFS was significantly longer ($p < 0.001$) in tumors with a TBR_{max} of < 2.0 (mean: 665 ± 32 days) compared to tumors with higher TBR_{max} (220 ± 39 days) (Fig. 4B). This arbitrary threshold was established by a retrospective data analysis. In the low TBR_{max} group, BSG was confirmed by histopathology in 4 of 7 patients.

4. Discussion

FET-PET is a continuously investigated imaging modality in adult patients with supratentorial gliomas, which might have the potential to become clinically established in the future [24]. However, the role of FET-PET in the comparably seldom adult brainstem gliomas has yet not been thoroughly investigated. Owing to their critical anatomical location, biopsy is rarely done, and adult BSG are mainly defined by their MR imaging appearance.

In our study, we aimed to characterize FET-PET features of adult BSG, depending on their histopathology and MR morphology, and with regard to the subsequent course of disease. We found no significant difference of FET-PET parameters among HGG and LGG, but progression-free survival was significantly longer in patients with tumors exhibiting a TBR_{max} of < 2.0.

An overlap of SUV_{max} and TBR_{max} values was described for supratentorial gliomas with different histological grading [17,34]. However, several studies indicated that at least HGG and LGG can be differentiated based on their TBR, with a cut-off of 2.5 used in the work by Rapp et al. [17]. The lack of a more detailed prediction of tumor grading is a known limitation of many amino acid tracers, and even absence of FET uptake in LGG might not indicate an indolent course of disease [35]. In our study, the TAC analysis revealed no significant difference between HGG and LGG. This is different to supratentorial gliomas, where such dynamic analyses were shown suitable for differentiating LGG and HGG in approximately two thirds of patients [14,32,34,35].

Obtaining histopathology is more challenging in BSG compared to supratentorial gliomas — and if biopsy is performed, often the specimen is not representative of the tumor grade, rendering the procedure inaccurate. Therefore, in lieu of histopathology, the MR appearance of BSG is taken as a substitute for grading purposes [8]. Nonetheless, MR features do not necessarily reflect the exact histopathological grade, both in supratentorial gliomas and BSG [36,37]. Rachinger et al. showed that the diagnostic value of conventional MR imaging in treatment planning of adult BSG is insufficient due to mismatches between imaging classification and histopathological grading [36]. In our study, we found that FET-PET parameters also cannot reliably characterize the grade of BSG. Similarly, Tscherpel et al. observed high FET uptake in a considerable number of actual low-grade BSG and spinal cord gliomas [19]. These findings might therefor reflect the intricate nature and intratumoral heterogeneity of BSG. Our findings are also in line with the results of Rosenfeld et al. who found no specific FET pattern in pediatric low-grade BSG [10].

We observed a more favorable course of BSG with a TBR_{max} of < 2.0 in our study. This finding might help identify individuals with either a poor or a favorable long-term prognosis, in order to optimize their long-term management — especially with regard to the timing of follow-up imaging. Our findings might also affect the short-term management of BSG patients: FET-PET may potentially obviate a risky invasive procedure, since it might identify more aggressive adult BSG in the absence of biopsy. However, this would need further substantiation by a study with a larger cohort of patients.

Floeth et al. reported that the most favorable prognosis for supratentorial LGG was associated with low FET uptake of these tumors (similar or less than surrounding brain tissue) [38]. Also Galldiks et al. showed in a prospective study that low TBR_{max} of glioblastoma multiforme is a significant predictor for progression-free survival and overall survival [39]. The same group showed that a TBR_{max} threshold of 2.0 might be able to separate recurrent/progressive gliomas from stable gliomas [23]. Tscherpel et al. provided evidence that FET-PET might be able to identify the time of progression in patients with BSG [19]. Our study additionally shows that FET-PET might be able to prognosticate the survival of BSG patients, with low amino acid uptake reflecting a better prognosis in a mixed population of high-grade and low-grade BSG. Notably, conventional MR imaging alone cannot predict the survival of patients with low-grade BSG [40]. Survival time of patients may be shortened if potentially progressive lesions are treated with delay, and vice versa, unnecessary treatment-related morbidity may be induced with too early or too aggressive treatment of stable lesions [38]. In supratentorial tumors, sufficient diagnostic accuracy of FET-PET still remains to be proven in order to influence therapeutic decisions. Histopathologic confirmation by biopsy or open surgery remains mandatory for adequate treatment decisions in supratentorial gliomas [36]. In BSG, which are far less amenable to biopsy, FET-PET might become a useful diagnostic adjunct for therapy decision making.

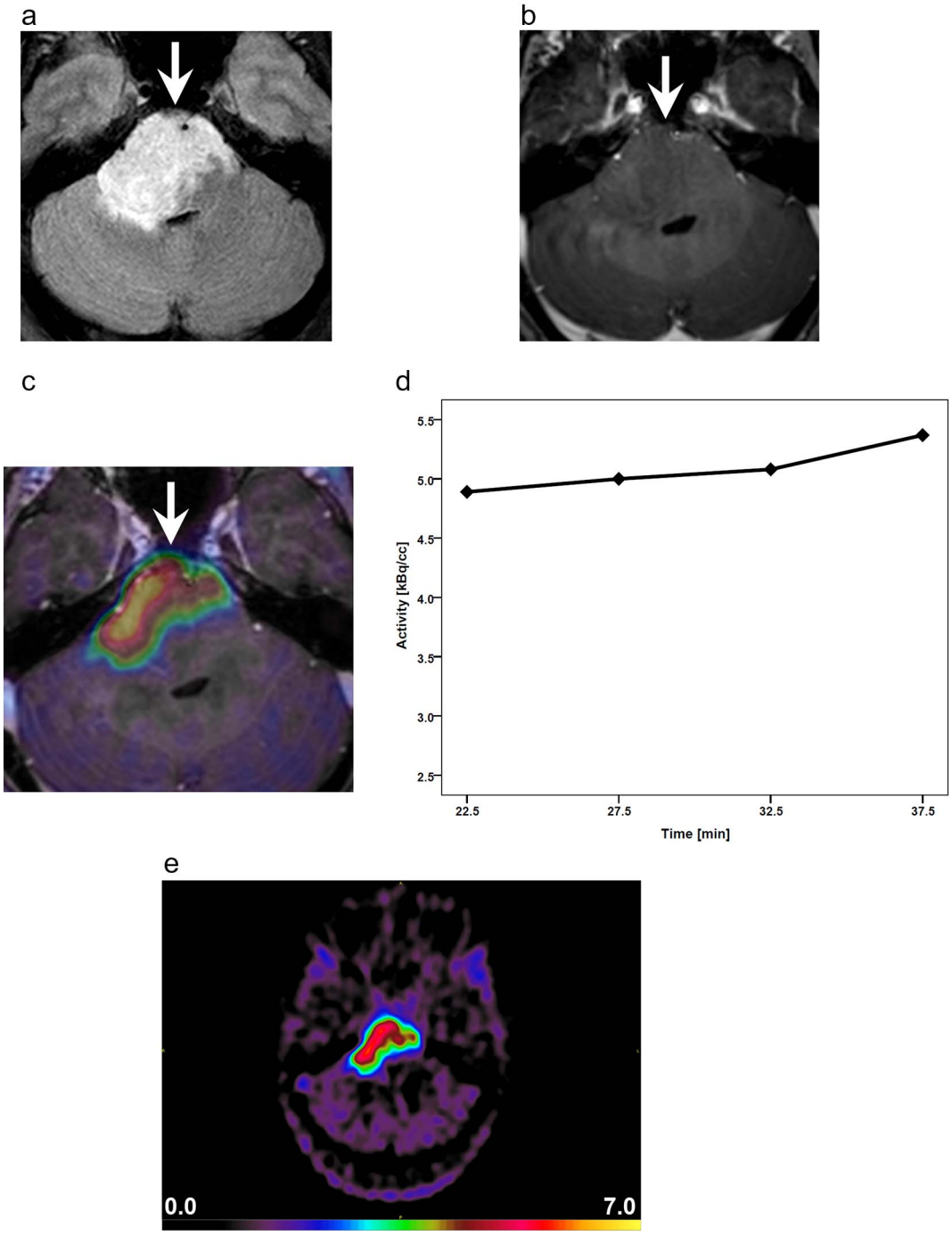

Fig. 1. 29 year-old female with diffuse intrinsic low-grade glioma. Axial fluid-attenuated inversion recovery (FLAIR) showing high signal intensity involving the right side of the pons (A, arrow). Absence of pathologic enhancement is seen on axial T1-weighted post-contrast image (B, arrow). Co-registered MR and FET-PET image demonstrates high FET uptake of the lesion (C, arrow; SUV_{max} 6.38, TBR_{max} 5.23). The time activity curve shows a wash-in pattern that does not reach a maximum (D). The FET-PET-only image (E) demonstrates the lesion together with an SUV scale.

4.1. Limitations

The longer PFS of BSG patients with a TBR_{max} of < 2.0 compared to BSG patients with a TBR_{max} of > 2.0 (665 ± 32 days versus 220 ± 39 days) was demonstrated using a Kaplan-Meier analysis. However, Kaplan-Meier analysis might be misleadingly instable due to low event number and flawed due to low patient number, which is a limitation of our study [41]. However, adult BSG are very rare tumors, and FET-PET is available mainly at tertiary care hospitals. Considering the scarcity of similar reports, multicentric studies may be advisable to expand our experience about the influence of FET-PET on the diagnosis of adult BSG. Another limitation is the rather mixed study cohort. However, all patients had brainstem gliomas and were stable at time of FET-PET imaging, serving as a common denominator. Other retrospective work on FET-PET in BSG was also conducted retrospectively in rather mixed cohorts [19]. This is likely due to the comparably low incidence of BSG. Nevertheless, our cohort did focus specifically on BSG and did not include other infratentorial entities or spinal cord gliomas as other studies. As an inherent bias of a retrospective study, the results of the FET-PET exam might have influenced clinical decisions and might have impacted e.g. on the timing and interval of follow-up consultations and imaging. However, the primary indication of all FET-PET

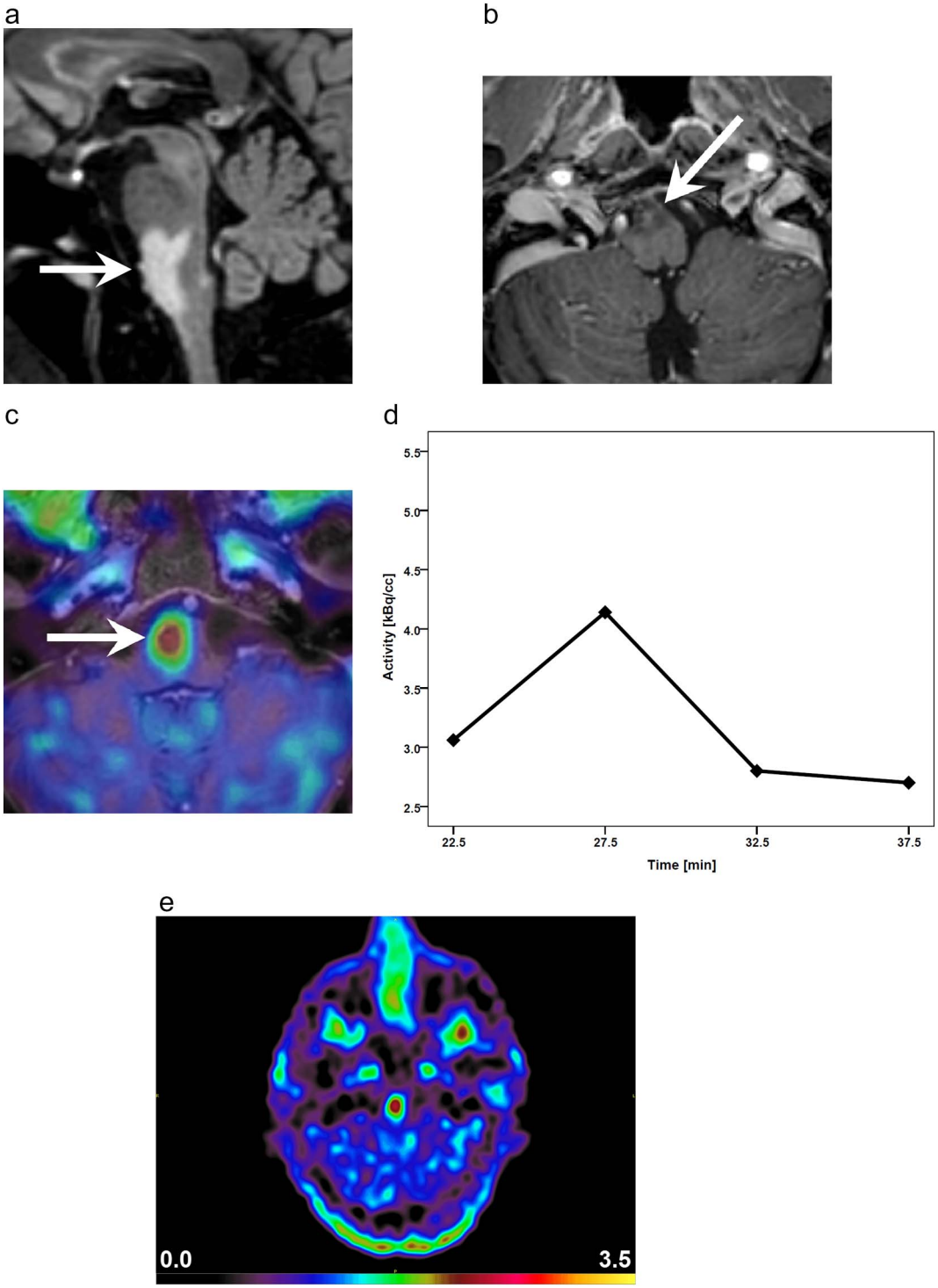

Fig. 2. 53 year-old male with an anaplastic astrocytoma. Sagittal fluid-attenuated inversion recovery (FLAIR) shows increased signal intensity involving the medulla oblongata and pons (A, arrow). Axial T1-weighted post-contrast image shows faint focal enhancement (B, arrow). Co-registered MR and FET-PET image demonstrates focal high uptake (C, arrow; SUV_{max} 2.37, TBR_{max} 2.11). The time activity curve shows peaking of the curve at an early time point, followed by a steep decrease (wash-out) (D). The FET-PET-only image (E) demonstrates the lesion together with an SUV scale.

exams analyzed in this study was to establish a baseline value in clinically stable patients, and not to determine a potential starting point for therapy. We acknowledge that FET-PET parameters did not match the different MR types and histopathological grades of adult BSG, but also the MR appearance of BSG does not allow a proper deduction of histopathology and grading [36,37]. Another limitation of our study is that we investigated the progression-free survival, which does not necessarily reflect the overall survival. In our cohort, the overall survival would not allow for a reliable conclusion, owing to the low number of deaths. Adult BSG are known to have a comparably fair prognosis. Besides, PFS is a generally accepted measure of outcome.

4.2. Conclusion

In conclusion, our study shows that FET-PET might eventually be able to prognosticate disease progression in adult BSG. SUV_{max} and

Table 4
FET-PET parameters in high grade gliomas and low grade gliomas, and in progressive gliomas and stable gliomas.

FET-PET parameter	HGG (n = 9)	LGG (n = 7)	*p*-Value	Progressive (n = 11)	Stable (n = 5)	*p*-Value
SUV_{max} (mean ± SD)	2.50 ± 1.04	3.26 ± 2.02	0.711	3.57 ± 1.47	1.60 ± 0.51	0.003
TBR_{max} (mean ± SD)	2.14 ± 0.73	2.69 ± 1.66	0.672	3.00 ± 1.12	1.36 ± 0.33	0.001
TAC pattern						
TAC pattern 1	0	2		2	0	
TAC pattern 2	2	3		3	2	
TAC pattern 3	7	2		6	3	
SoD (mean ± SD)	0.05 ± 0.41	0.08 ± 0.33	0.491	0.09 ± 0.44	0.02 ± 0.21	0.828

Note — FET, ^{18}F-fluoro-ethyl-tyrosine; HGG, high-grade glioma; LGG, low-grade glioma; SD, standard deviation; SoD, sum of differences; SUV_{max}, maximum standardized uptake value; TAC, time activity curve; TBR_{max}, tumor-to-brain ratio.

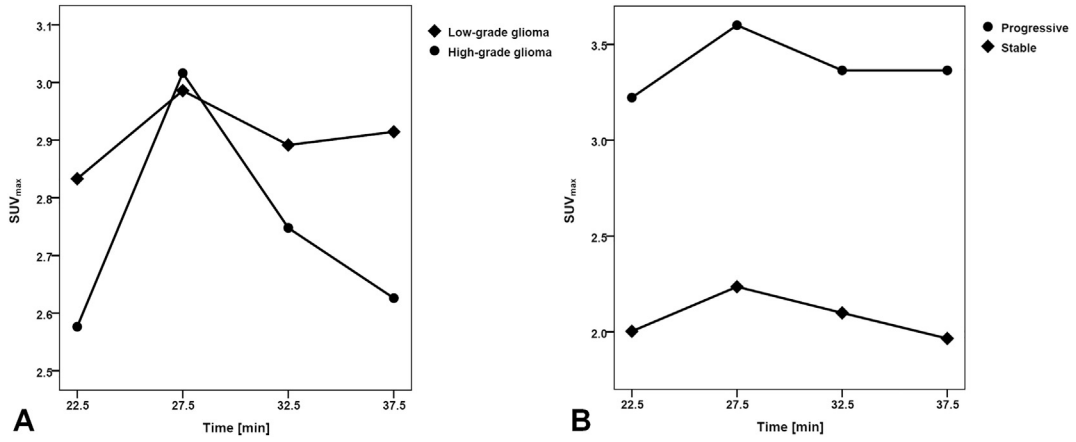

Fig. 3. Time activity curves (TAC) for high-grade gliomas (n = 9) and low-grade gliomas (n = 7) (A), and progressive gliomas (n = 11) and stable gliomas (n = 5) (B). A peaking of the curve at time point (t) 2 at 27.5 min was evident in high-grade gliomas, but uptake was not significantly different between high-grade gliomas and low-grade gliomas at any time point of the TAC (*p*-values: 0.758 (t1), 1.000 (t2), 0.918 (t3), 0.758 (t4) (A). Progressive gliomas had significantly higher uptake at any time point of the TAC than stable gliomas (*p*-values: 0.003 (t1), 0.007 (t2), 0.007 (t3), 0.005 (t4).

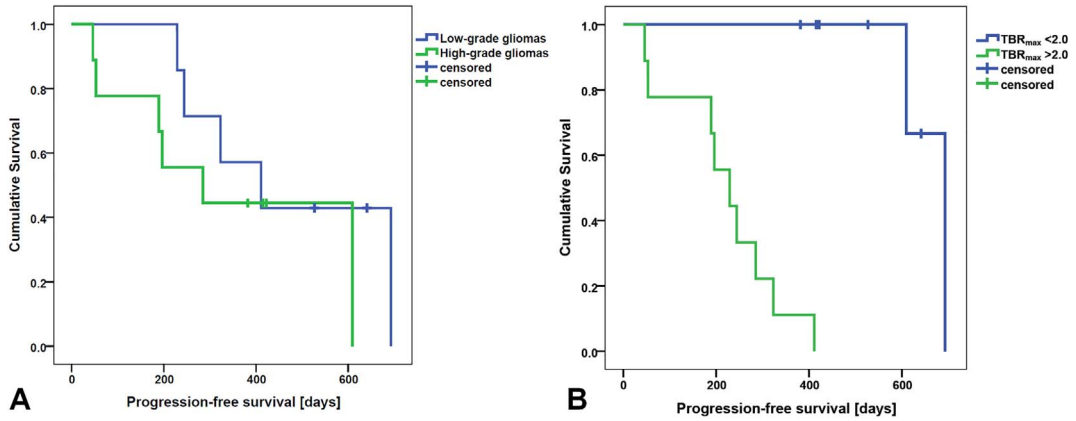

Fig. 4. Kaplan-Meier analysis of progression-free survival. PFS was similar for high-grade gliomas (n = 9) and low-grade gliomas (n = 7) (A, $p = 0.358$). PFS was significantly longer ($p < 0.001$) in tumors with a TBR_{max} of < 2.0 (n = 7) compared to tumors with a TBR_{max} of > 2.0 (n = 9) (B).

TBR_{max} are higher in progressive gliomas than in stable gliomas. Tumors with a TBR_{max} of > 2.0 might be associated with earlier disease progression, whereas patients with tumors exhibiting a TBR_{max} of < 2.0 might experience longer progression-free survival. Since our cohort was rather small, studies with a larger patient population are needed to further establish the role of FET-PET imaging in BSG patients, especially with regard to survival.

5. Compliance with ethical standards

The institution of the authors A.A.A., A.T.A., A.A., P.S., A.B., P.V.-H., and M.W.H. has received grants from GE Healthcare. However, no direct funding was received for this study. S.K. declares no conflicts of interest. All procedures performed were in accordance with the ethical standards of the institutional research committee and with the 1964 Helsinki declaration and its later amendments. Informed consent was obtained from all individual participants included in the study, except where waived by the ethical committee (see Material and methods section).

Conflict of interests

The institution of the authors A.A.A., A.T.A., A.A., I.A.B., P.S., A.B., P.V.-H., and M.W.H. has received grants from GE Healthcare. However, no direct funding was received for this study. S.K. declares no conflicts of interest.

References

[1] Barkovich AJ, Krischer J, Kun LE, Packer R, Zimmerman RA, Freeman CR, et al. Brain stem gliomas: a classification system based on magnetic resonance imaging. Pediatr Neurosurg 1990;16(2):73–83.

[2] Dodo T, Okada T, Yamamoto A, Kanagaki M, Fushimi Y, Okada T, et al. T1-weighted MR imaging of glioma at 3 T: a comparative study of 3D MPRAGE vs. conventional 2D spin-echo imaging. Clin Imaging 2016;40(6):1257–61.

[3] Grimm SA, Chamberlain MC. Brainstem glioma: a review. Curr Neurol Neurosci Rep 2013;13(5):346.

[4] Landolfi JC, Thaler HT, DeAngelis LM. Adult brainstem gliomas. Neurology 1998;51(4):1136–9.

[5] Lachi PK, Irrakula M, Ahmed SF, Joseph D, Pamidighantam S, Jagannath Rao Naidu KV. Clinical profile and outcomes in brainstem glioma: an institutional experience. Asian J Neurosurg 2015;10(4):298–302.

[6] Guillamo JS, Monjour A, Taillandier L, Devaux B, Varlet P, Haie-Meder C, et al. Brainstem gliomas in adults: prognostic factors and classification. Brain 2001;124(Pt 12):2528–39.

[7] Cha S. Neuroimaging in neuro-oncology. Neurotherapeutics 2009;6(3):465–77.

[8] Purohit B, Kamli AA, Kollias SS. Imaging of adult brainstem gliomas. Eur J Radiol 2015;84(4):709–20.

[9] Reyes-Botero G, Mokhtari K, Martin-Duverneuil N, Delattre JY, Laigle-Donadey F. Adult brainstem gliomas. Oncologist 2012;17(3):388–97.

[10] Rosenfeld A, Etzl M, Bandy D, Carpenteri D, Gieseking A, Dvorchik I, et al. Use of positron emission tomography in the evaluation of diffuse intrinsic brainstem gliomas in children. J Pediatr Hematol Oncol 2011;33(5):369–73.

[11] Tisnado J, Young R, Peck KK, Haque S. Conventional and advanced imaging of diffuse intrinsic pontine glioma. J Child Neurol 2016;31(12):1386–93.

[12] Zukotynski KA, Fahey FH, Kocak M, Alavi A, Wong TZ, Treves ST, et al. Evaluation of ^{18}F-FDG PET and MRI associations in pediatric diffuse intrinsic brain stem glioma: a report from the Pediatric Brain Tumor Consortium. J Nucl Med 2011;52(2):188–95.

[13] Rachinger W, Goetz C, Popperl G, Gildehaus FJ, Kreth FW, Holtmannspotter M, et al. Positron emission tomography with O-(2-[^{18}F]fluoroethyl)-L-tyrosine versus magnetic resonance imaging in the diagnosis of recurrent gliomas. Neurosurgery 2005;57(3):505–11. discussion-11.

[14] Weckesser M, Langen KJ, Rickert CH, Kloska S, Straeter R, Hamacher K, et al. O-(2-[^{18}F]fluorethyl)-L-tyrosine PET in the clinical evaluation of primary brain tumours. Eur J Nucl Med Mol Imaging 2005;32(4):422–9.

[15] Meric K, Killeen RP, Abi-Ghanem AS, Soliman F, Novruzov F, Cakan E, et al. The use of ^{18}F-FDG PET ratios in the differential diagnosis of common malignant brain tumors. Clin Imaging 2015;39(6):970–4.

[16] Tawakol A, Migrino RQ, Bashian GG, Bedri S, Vermylen D, Cury RC, et al. In vivo ^{18}F-fluorodeoxyglucose positron emission tomography imaging provides a non-invasive measure of carotid plaque inflammation in patients. J Am Coll Cardiol 2006;48(9):1818–24.

[17] Rapp M, Heinzel A, Galldiks N, Stoffels G, Felsberg J, Ewelt C, et al. Diagnostic performance of ^{18}F-FET PET in newly diagnosed cerebral lesions suggestive of glioma. J Nucl Med 2013;54(2):229–35.

[18] Pauleit D, Floeth F, Hamacher K, Riemenschneider MJ, Reifenberger G, Muller HW, et al. O-(2-[^{18}F]fluoroethyl)-L-tyrosine PET combined with MRI improves the diagnostic assessment of cerebral gliomas. Brain 2005;128(Pt 3):678–87.

[19] Tscherpel C, Dunkl V, Ceccon G, Stoffels G, Judov N, Rapp M, et al. The use of O-(2-^{18}F-fluoroethyl)-L-tyrosine PET in the diagnosis of gliomas located in the brainstem and spinal cord. Neuro Oncol 2017;19(5):710–8.

[20] Herholz K. Brain tumors: an update on clinical PET research in gliomas. Semin Nucl Med 2017;47(1):5–17.

[21] Ellingson BM, Wen PY, Cloughesy TF. Modified criteria for radiographic response assessment in glioblastoma clinical trials. Neurotherapeutics 2017;14(2):307–20.

[22] van den Bent MJ, Wefel JS, Schiff D, Taphoorn MJ, Jaeckle K, Junck L, et al. Response assessment in neuro-oncology (a report of the RANO group): assessment of outcome in trials of diffuse low-grade gliomas. Lancet Oncol 2011;12(6):583–93.

[23] Galldiks N, Stoffels G, Filss C, Rapp M, Blau T, Tscherpel C, et al. The use of dynamic O-(2-^{18}F-fluoroethyl)-L-tyrosine PET in the diagnosis of patients with progressive and recurrent glioma. Neuro Oncol 2015;17(9):1293–300.

[24] Dunet V, Rossier C, Buck A, Stupp R, Prior JO. Performance of ^{18}F-fluoro-ethyl-tyrosine (^{18}F-FET) PET for the differential diagnosis of primary brain tumor: a systematic review and metaanalysis. J Nucl Med 2012;53(2):207–14.

[25] Burger C, Buck A. Quantifying PET. In: von Schulthess GK, editor. Molecular anatomic imaging. Philadelphia: Lippincott Williams & Wilkins; 2007. p. 85–9.

[26] Laffon E, Lamare F, de Clermont H, Burger IA, Marthan R. Variability of average SUV from several hottest voxels is lower than that of SUVmax and SUVpeak. Eur Radiol 2014;24(8):1964–70.

[27] Burger IA, Huser DM, Burger C, von Schulthess GK, Buck A. Repeatability of FDG quantification in tumor imaging: averaged SUVs are superior to SUVmax. Nucl Med Biol 2012;39(5):666–70.

[28] Langen KJ, Bartenstein P, Boecker H, Brust P, Coenen HH, Drzezga A, et al. German guidelines for brain tumour imaging by PET and SPECT using labelled amino acids. Nuklearmedizin 2011;50(4):167–73.

[29] Sadeghi N, Salmon I, Decaestecker C, Levivier M, Metens T, Wikler D, et al. Stereotactic comparison among cerebral blood volume, methionine uptake, and histopathology in brain glioma. AJNR Am J Neuroradiol 2007;28(3):455–61.

[30] Popperl G, Gotz C, Rachinger W, Gildehaus FJ, Tonn JC, Tatsch K. Value of O-(2-[^{18}F]fluoroethyl)-L-tyrosine PET for the diagnosis of recurrent glioma. Eur J Nucl Med Mol Imaging 2004;31(11):1464–70.

[31] Calcagni ML, Galli G, Giordano A, Taralli S, Anile C, Niesen A, et al. Dynamic O-(2-[^{18}F]fluoroethyl)-L-tyrosine (F-18 FET) PET for glioma grading: assessment of individual probability of malignancy. Clin Nucl Med 2011;36(10):841–7.

[32] Popperl G, Kreth FW, Herms J, Koch W, Mehrkens JH, Gildehaus FJ, et al. Analysis of ^{18}F-FET PET for grading of recurrent gliomas: is evaluation of uptake kinetics superior to standard methods? J Nucl Med 2006;47(3):393–403.

[33] Louis DN, Ohgaki H, Wiestler OD, Cavenee WK, Burger PC, Jouvet A, et al. The 2007 WHO classification of tumours of the central nervous system. Acta Neuropathol 2007;114(2):97–109.

[34] Jansen NL, Graute V, Armbruster L, Suchorska B, Lutz J, Eigenbrod S, et al. MRI-suspected low-grade glioma: is there a need to perform dynamic FET PET? Eur J Nucl Med Mol Imaging 2012;39(6):1021–9.

[35] Dunet V, Maeder P, Nicod-Lalonde M, Lhermitte B, Pollo C, Bloch J, et al. Combination of MRI and dynamic FET PET for initial glioma grading. Nuklearmedizin 2014;53(4):155–61.

[36] Rachinger W, Grau S, Holtmannspotter M, Herms J, Tonn JC, Kreth FW. Serial stereotactic biopsy of brainstem lesions in adults improves diagnostic accuracy compared with MRI only. J Neurol Neurosurg Psychiatry 2009;80(10):1134–9.

[37] Dellaretti M, Touzet G, Reyns N, Dubois F, Gusmao S, Pereira JL, et al. Correlation among magnetic resonance imaging findings, prognostic factors for survival, and histological diagnosis of intrinsic brainstem lesions in children. J Neurosurg Pediatr 2011;8(6):539–43.

[38] Floeth FW, Pauleit D, Sabel M, Stoffels G, Reifenberger G, Riemenschneider MJ, et al. Prognostic value of O-(2-^{18}F-fluoroethyl)-L-tyrosine PET and MRI in low-grade glioma. J Nucl Med 2007;48(4):519–27.

[39] Galldiks N, Langen KJ, Holy R, Pinkawa M, Stoffels G, Nolte KW, et al. Assessment of treatment response in patients with glioblastoma using O-(2-^{18}F-fluoroethyl)-L-tyrosine PET in comparison to MRI. J Nucl Med 2012;53(7):1048–57.

[40] Hargrave D, Chuang N, Bouffet E. Conventional MRI cannot predict survival in childhood diffuse intrinsic pontine glioma. J Neurooncol 2008;86(3):313–9.

[41] Simon R, Altman DG. Statistical aspects of prognostic factor studies in oncology. Br J Cancer 1994;69(6):979–85.